

NOVEL IN-LINE MICROSTRIP COUPLED-LINE BANDSTOP FILTER WITH SHARP SKIRT SELECTIVITY

Gui Liu^{1, *} and Yongle Wu²

¹College of Physics & Electronic Information Engineering, Wenzhou University, Wenzhou, Zhejiang, China

²School of Electronic Engineering, Beijing University of Posts and Telecommunications, Beijing, China

Abstract—This paper presents a novel design approach to design in-line microstrip bandstop filter with accurate design theory and sharp skirt selectivity. This kind of bandstop filter is based on a simple coupled-line structure, indicating compact and flexible circuit layout for microstrip implementation. For a single-section bandstop filter, the scattering parameters and their constrain conditions are achieved, which provides an effective design guide for multi-section bandstop filters. Theoretical analysis indicates that the even-mode and odd-mode characteristic impedances can be easily used to determine the desired bandstop performance while the total circuit layout keeps very compact. For demonstration, seven numerical examples are designed, calculated, and compared. Finally, both experimental and simulation results of a two-section two-cell microstrip bandstop filter operating at 1 GHz are presented to verify the theoretical predications.

1. INTRODUCTION

Bandstop filters are preferred in many applications since they can relax the strict requirement for bandpass filter selectivity such as presenting much stronger interference. In addition, bandstop filters are used in many active circuits as RF chokes [1]. The simplest form of a bandstop filter may just consist of a parallel open-circuit transmission-line stub, which is often found in many systems. For more selective performance, more elements are required. However, the circuit size for such a high-selectivity bandstop filter becomes very large. Therefore, developing a

Received 19 January 2013, Accepted 25 February 2013, Scheduled 6 March 2013

* Corresponding author: Gui Liu (iitgliu2@gmail.com).

novel and compact microstrip bandstop filter with a simple structure and sharp skirt selectivity becomes very necessary.

Recently, various implementation techniques of microstrip bandstop filters have been utilized. These developed bandstop filters include dual-band or multi-band bandstop filters [2–6] and tunable bandstop filters with special features [7–9]. Usually, the distributed elements including transmission-line, coupled-line sections and lumped elements are used in the design of bandstop filters. Among them, coupled-line sections, which are applied in bandpass filters [10] and impedance transformers [11], have several advantages such as compact size and flexible circuit parameters. Also, based on two meandered parallel-coupled lines, compact bandstop filters have been reported in [12, 13], but this structure is *not an in-line form*. Another compact bandstop filter with a coupled-line structure is presented in [14], stopband rejection depth and bandwidth can be controlled easily, and however, *additional* open-circuit transmission-line stubs are required. In [15], a novel complementary split ring resonators defected microstrip structure is introduced to design a microstrip bandstop filter. But the analytical theory for direct synthesis *is not complete*. Meanwhile, although novel designs of a wide spurious-free planar bandstop filter using coupled-line sections have been proposed in [16, 17], the complicated transmission-line stubs are necessary in [16] while the stop-band bandwidth and selectivity performance need to be improved in [17].

In this paper, a novel approach is proposed to design bandstop filter with sharp skirt selectivity and compact size. This bandstop filter is based on lossless coupled-line models. Due to its simplification, the closed-form expressions for the scattering parameters of such a bandstop filter can be easily obtained. The operating bandwidth analysis and typical numerical examples are provided. Theoretical predictions are validated by full-wave simulation and measurement of a fabricated microstrip bandstop filter. The measured results show that the return loss is larger than 20 dB from 0.88 to 1.11 GHz. The pass-band insertion loss is smaller than 0.66 dB in the range of 0 to 0.67 GHz and smaller than 1.91 dB in the range of 1.24 to 2.6 GHz.

2. CIRCUIT STRUCTURE AND DESIGN THEORY

Figure 1 shows the proposed single-section coupled-line bandstop filter. This basic unit cell contains a parallel coupled line with even-mode (odd-mode) characteristic impedance of Z_e (Z_o) and electrical length of θ_c . The voltages and currents are defined in Figure 1. According to the given mathematical results [1, 11], the impedance matrix elements

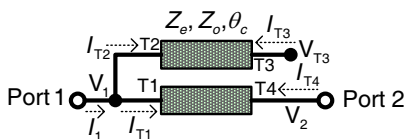


Figure 1. The unit cell with circuit parameter definition of the proposed coupled-line bandstop filters.

for the terminal impedances (T1,T2,T3,T4) are given by

$$Z_{T1T1} = Z_{T2T2} = Z_{T3T3} = Z_{T4T4} = -j \left(\frac{Z_e + Z_o}{2} \right) \cot(\theta_c) = \frac{-jZ_a}{\tan(\theta_c)} \quad (1a)$$

$$Z_{T1T2} = Z_{T2T1} = Z_{T3T4} = Z_{T4T3} = -j \left(\frac{Z_e - Z_o}{2} \right) \cot(\theta_c) = \frac{-jZ_b}{\tan(\theta_c)} \quad (1b)$$

$$Z_{T1T3} = Z_{T3T1} = Z_{T2T4} = Z_{T4T2} = -j \left(\frac{Z_e - Z_o}{2 \sin(\theta_c)} \right) = \frac{-jZ_b}{\sin(\theta_c)} \quad (1c)$$

$$Z_{T1T4} = Z_{T4T1} = Z_{T2T3} = Z_{T3T2} = -j \left[\frac{Z_e + Z_o}{2 \sin(\theta_c)} \right] = \frac{-jZ_a}{\sin(\theta_c)} \quad (1d)$$

where

$$\begin{cases} Z_a = \frac{Z_e + Z_o}{2} \\ Z_b = \frac{Z_e - Z_o}{2} \end{cases} \quad (2)$$

Based on the definition of impedance matrix, the rigorous relationship between given voltages and currents is expressed by

$$V_1 = Z_{T1T1}I_{T1} + Z_{T1T2}I_{T2} + Z_{T1T3}I_{T3} + Z_{T1T4}I_{T4} \quad (3a)$$

$$V_1 = Z_{T2T1}I_{T1} + Z_{T2T2}I_{T2} + Z_{T2T3}I_{T3} + Z_{T2T4}I_{T4} \quad (3b)$$

$$V_{T3} = Z_{T3T1}I_{T1} + Z_{T3T2}I_{T2} + Z_{T3T3}I_{T3} + Z_{T3T4}I_{T4} \quad (3c)$$

$$V_2 = Z_{T4T1}I_{T1} + Z_{T4T2}I_{T2} + Z_{T4T3}I_{T3} + Z_{T4T4}I_{T4} \quad (3d)$$

In addition, for this special circuit configuration shown in Fig. 1(a), other necessary conditions are

$$\begin{cases} I_1 = I_{T1} + I_{T2} \\ I_2 = I_{T4} \\ I_{T3} = 0 \end{cases} \quad (4)$$

From (3) and (4), the following equations can be established:

$$V_1 = Z_{T1T1}I_{T1} + Z_{T1T2}(I_1 - I_{T1}) + Z_{T1T4}I_2 \quad (5a)$$

$$V_1 = Z_{T2T1}I_{T1} + Z_{T2T2}(I_1 - I_{T1}) + Z_{T2T4}I_2 \quad (5b)$$

$$V_2 = Z_{T4T1}I_{T1} + Z_{T4T2}(I_1 - I_{T1}) + Z_{T4T4}I_2 \quad (5c)$$

Equating the Equations (5a) and (5b) results in

$$\begin{aligned} & Z_{T_2T_1}I_{T_1} + Z_{T_2T_2}(I_1 - I_{T_1}) + Z_{T_2T_4}I_2 \\ &= Z_{T_1T_1}I_{T_1} + Z_{T_1T_2}(I_1 - I_{T_1}) + Z_{T_1T_4}I_2 \end{aligned} \tag{6}$$

The mathematical expressions of I_{T_1} can be achieved as

$$I_{T_1} = \frac{(Z_{T_1T_2} - Z_{T_2T_2}) I_1 + (Z_{T_1T_4} - Z_{T_2T_4}) I_2}{(Z_{T_2T_1} + Z_{T_1T_2} - Z_{T_2T_2} - Z_{T_1T_1})} \tag{7}$$

Inserting (7) into (5), and after simplification, we have

$$V_1 = \frac{(Z_{T_2T_1}Z_{T_1T_2} - Z_{T_2T_2}Z_{T_1T_1})I_1 + (Z_{T_2T_1} - Z_{T_2T_2})(Z_{T_1T_4} - Z_{T_2T_4})I_2}{(Z_{T_2T_1} + Z_{T_1T_2} - Z_{T_2T_2} - Z_{T_1T_1})} \tag{8a}$$

$$V_2 = \frac{(Z_{T_4T_1} + Z_{T_4T_2})(Z_{T_1T_2} - Z_{T_2T_2}) I_1 + (Z_{T_4T_1}^2 + Z_{T_4T_2}^2 - 2Z_{T_4T_1}Z_{T_2T_4} + 2Z_{T_4T_4}Z_{T_2T_1} - 2Z_{T_4T_4}Z_{T_2T_2}) I_2}{(Z_{T_2T_1} + Z_{T_1T_2} - Z_{T_2T_2} - Z_{T_1T_1})} \tag{8b}$$

Thus, from (8), the elements of impedance (Z) matrix for the ports 1 and 2 shown in Figure 1 can be extracted as

$$\begin{cases} Z_{11} = \frac{(Z_{T_2T_1}Z_{T_1T_2} - Z_{T_2T_2}Z_{T_1T_1})}{2(Z_{T_2T_1} - Z_{T_1T_1})} \\ Z_{12} = \frac{(Z_{T_2T_1} - Z_{T_2T_2})(Z_{T_1T_4} + Z_{T_2T_4})}{2(Z_{T_2T_1} - Z_{T_1T_1})} \\ Z_{21} = \frac{(Z_{T_4T_1} + Z_{T_4T_2})(Z_{T_1T_2} - Z_{T_2T_2})}{2(Z_{T_2T_1} - Z_{T_1T_1})} \\ Z_{22} = \frac{(Z_{T_4T_1}^2 + Z_{T_4T_2}^2 - 2Z_{T_4T_1}Z_{T_2T_4} + 2Z_{T_4T_4}Z_{T_2T_1} - 2Z_{T_4T_4}Z_{T_2T_2})}{2(Z_{T_2T_1} - Z_{T_1T_1})} \end{cases} \tag{9}$$

Finally, according to the results about scattering parameters in terms of impedance (Z) parameters [1], the scattering parameters of this bandstop filter shown in Figure 1 can be calculated by

$$\begin{cases} S_{11} = \frac{(Z_{11} - R_o)(Z_{22} + R_o) - Z_{12}Z_{21}}{(Z_{11} + R_o)(Z_{22} + R_o) - Z_{12}Z_{21}} \\ S_{12} = \frac{2Z_{12}R_o}{(Z_{11} + R_o)(Z_{22} + R_o) - Z_{12}Z_{21}} \\ S_{21} = \frac{2Z_{21}R_o}{(Z_{11} + R_o)(Z_{22} + R_o) - Z_{12}Z_{21}} \\ S_{22} = \frac{(Z_{11} + R_o)(Z_{22} - R_o) - Z_{12}Z_{21}}{(Z_{11} + R_o)(Z_{22} + R_o) - Z_{12}Z_{21}} \end{cases} \tag{10}$$

where R_o is the port impedance. For a bandstop filter, the desired parameters should be constrained by

$$\begin{cases} S_{21} = 0, & \text{at } f_0 \\ S_{11} = 0, & \text{other frequencies} \end{cases} \tag{11}$$

where f_0 is the center frequency of bandstop filter. From the Equation (10), it can be observed that the condition $Z_{21} = 0$ can

be obtained when $S_{21} = 0$ is required. The corresponding relationship can be written as

$$(Z_{T4T1} + Z_{T4T2})(Z_{T1T2} - Z_{T2T2}) = 0 \quad (12)$$

By using (1) and (2), the Equation (12) can be simplified as

$$\frac{Z_e Z_o}{\sin^2(\theta_c)} \cos(\theta_c) = 0 \quad (13)$$

Therefore, for a desired band-stop filter operating at f_0 , the electrical length should satisfy

$$\theta_c = 0.5\pi, \text{ at } f_0 \quad (14)$$

For the following convenient explanation, the coupling coefficient C and equivalent characteristic impedance Z_T of the applied coupled-line section are defined by [1]

$$\begin{cases} C = \frac{Z_e - Z_o}{Z_e + Z_o} \\ Z_T = \sqrt{Z_e Z_o} \end{cases} \quad (15)$$

For this proposed bandstop filter, the band-edge frequencies to the **10-dB** return loss are f_{\max} and f_{\min} . Thus, the fractional bandwidth (FBW) is defined by [1]

$$FBW = 2 \frac{f_{\max} - f_{\min}}{f_{\max} + f_{\min}} \quad (16)$$

The variation of the **FBW** versus coupling coefficient C and equivalent characteristic impedance Z_T , computed from (10), (15), and (16), is plotted in Figures 2(a) and (b), respectively. The **FBW** is decreased when the coupling coefficient C is increased from -40 to -5 dB for each value of Z_T , as shown in Figure 2(a). From Figure 2(b), it can be seen that the **FBW** remains similar when the equivalent characteristic impedance Z_T ranges from 40 to 80Ω . Without loss of generality, two examples, namely, **Example A** and **Example B** are chosen from the design graph shown in Figure 2(b). Their theoretical responses are calculated by lossless coupled-line models and the corresponding results are shown in Figure 3. It is observed that the **Example A** has the equivalent characteristic impedance of $Z_T = 50 \Omega$ and the coupling coefficient of $C = -20$ dB. The **Example B** has the same value of the equivalent characteristic impedance but different value of the coupling coefficient $C = -8$ dB as Example A. From Figure 3, it can be observed that **FBW** of the **Example B** is smaller than that of the **Example A**, which keeps the same with the results in Figures 2(a) and 2(b).

The unit cell of the proposed bandstop filter is named as single-section single-cell bandstop filter. From Figure 3, we can find that

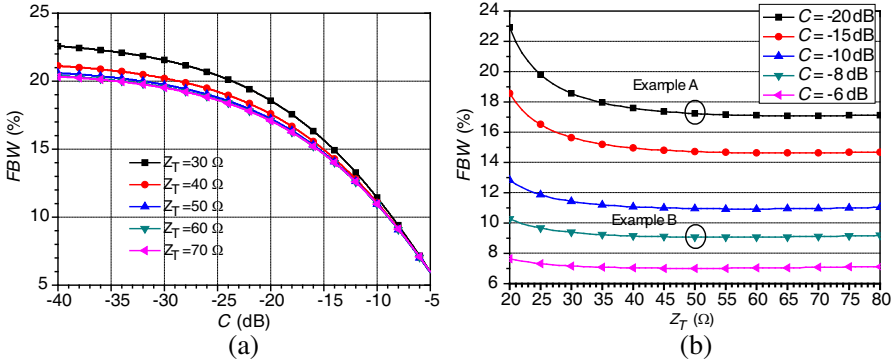


Figure 2. The bandwidth performance of the proposed single-section single-cell bandstop filter: (a) FBW versus coupling coefficient C ; (b) FBW versus equivalent characteristic impedance Z_T .

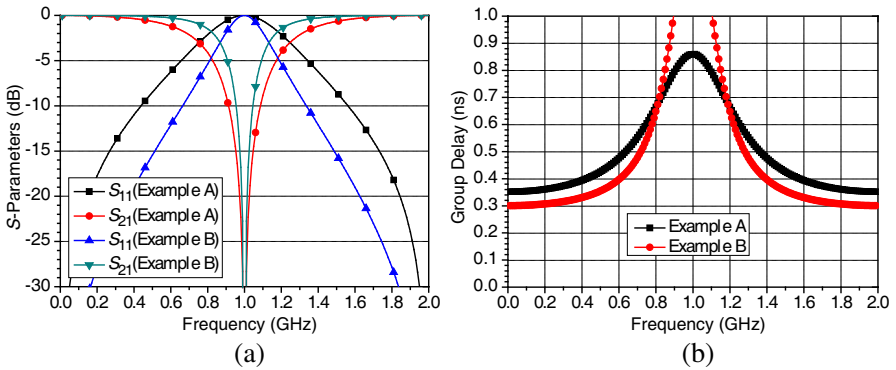


Figure 3. (a) The calculated scattering parameter and (b) group delay performance of the proposed single-section single-cell bandstop filter.

the stop band selectivity is not very good. Here, a novel single-section two-cell bandstop filter is constructed by parallel connected two unit cell. This structure does not increase the transmission distance compared to the single-section single-cell bandstop filter shown in Figure 1. The final circuit configuration is shown in Figure 4. Based on this proposed single-section two-cell bandstop filter, two examples, namely, **Example C** and **Example D** are chosen to present the responses. The equivalent characteristic impedance of both the **Example C** and **Example D** is $Z_T = 100 \Omega$. The coupling coefficients of the **Example C** and **Example D** are $C = -20$ dB and

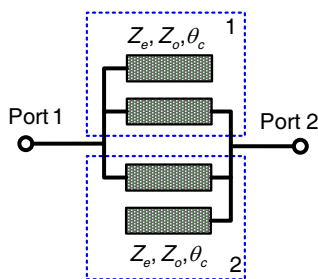


Figure 4. The circuit structure of the proposed single-section two-cell parallel coupled-line bandstop filter.

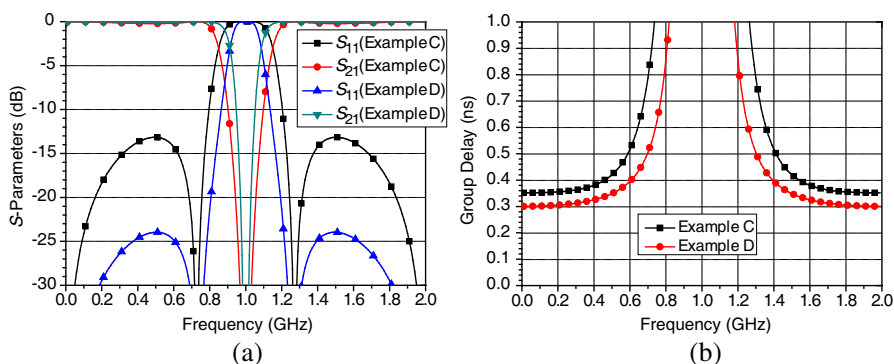


Figure 5. (a) The scattering parameter and (b) group delay performance of the proposed single-section two-cell parallel coupled-line bandstop filter.

-8 dB, respectively. As shown in Figure 5 although the *FBW* of the **Example D** is smaller than that of the **Example C**, the return loss in the pass band is *larger* than 23 dB for the **Example D** but the return loss at the pass band is *smaller* than 15 dB for the **Example C**. It is interesting that the stop band selectivity of both the **Example C** and **Example D** is excellent.

To obtain the desirable bandstop filters with high selectivity, a two-section two-cell coupled-line structure is proposed by using two previous structures shown in Figure 4. Figure 6 shows the final circuit structure. Because this proposed bandstop filter has four coupled-line sections, the total configuration looks like an in-line bandstop filtering transmission line, indicating a novel size-miniaturization filter. For the proposed two-section two-cell coupled-line bandstop filter, three examples including **Examples E, F, and G** are demonstrated. The equivalent characteristic impedance of the all **Examples E, F, G**

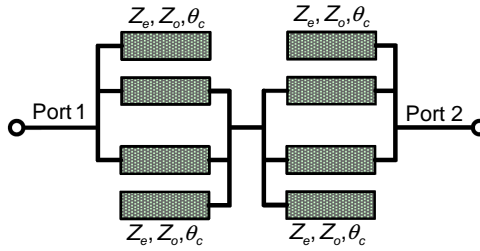


Figure 6. The final circuit structure of the proposed two-section two-cell coupled-line bandstop filter.

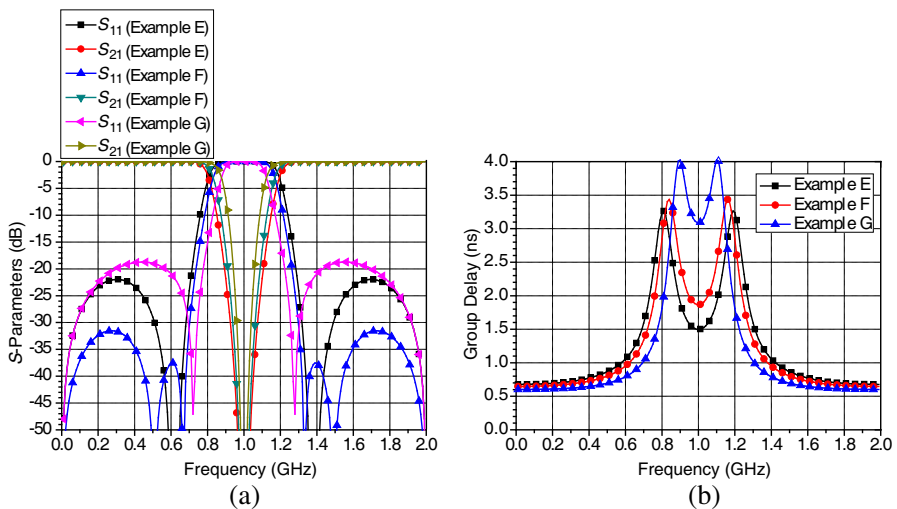


Figure 7. (a) The calculated scattering parameters and (b) group delay performance of the proposed two-section two-cell coupled-line bandstop filter.

is $Z_T = 122 \Omega$. The coupling coefficients of the **Examples E**, **F**, **G** are $C = -20$ dB, $C = -14$ dB and $C = -8$ dB, respectively. The calculated scattering parameters of these three examples are illustrated in Figure 7(a). The group delays of these three examples are compared in Figure 7(b). Obviously, the pass-band return loss and group delay of **Example F** are best among these three examples. The pass-band return loss is larger than 30 dB as shown in Figure 7(a) while the variation of the group delay is smallest among them, as shown in Figure 7(b). Note that the sharp skirt selectivity in the stop band (near 1 GHz) can be clearly observed from Figure 7 for **Examples E**, **F**, and **G**.

3. FULL-WAVE SIMULATION AND MEASUREMENT

In the previous section, it can be found that the scattering-parameter and group-delay performance of the **Example F** is best among the Examples A, B, C, D, E, F, and G. Therefore, similar (but not equal) to the circuit parameters of the **Example F**, another two-section two-cell coupled-line bandstop filter example is chosen for experimental verification. This chosen example has the even-mode characteristic impedance of $Z_e = 150 \Omega$ and the odd-mode characteristic impedance of $Z_o = 99 \Omega$. The electrical length is $\theta_c = 90^\circ$ at 1 GHz. The calculated responses of this chosen example are shown in Figure 8. Note that there are four reflection zeros in the upper pass band from 1.27 to 2.6 GHz while the variation of the calculated group delay is smaller than 1 ns in the low pass band from 0 to 0.7 GHz (The PA area in Figure 8(b)) and the upper pass band from 1.3 to 2.6 GHz (The PB area in Figure 8(b)).

For full-wave simulation (Sonnet EM simulator) and measurement, this chosen example is fabricated on a Rogers R04350 B with a dielectric constant of 3.48 and thickness of 0.762 mm. The microstrip layout of this chosen bandstop filter is shown in Figure 9. The dimensions (unit: mm) are easily determined as follows: $W_M = 1.72$, $W_1 = 0.22$, $W_2 = 0.26$, $S_1 = 0.6$, $S_2 = 0.44$, $S_3 = 0.26$, $L_1 = 48$, and $L_M = 7.5$. The total circuit layout is simulated by a numerical full-wave MoM method. Figure 10 shows the simulated responses of this microstrip bandstop filter example. The band-stop feature and good band-pass performance agrees with the predicted result.

The photograph of the fabricated bandstop filter is shown in

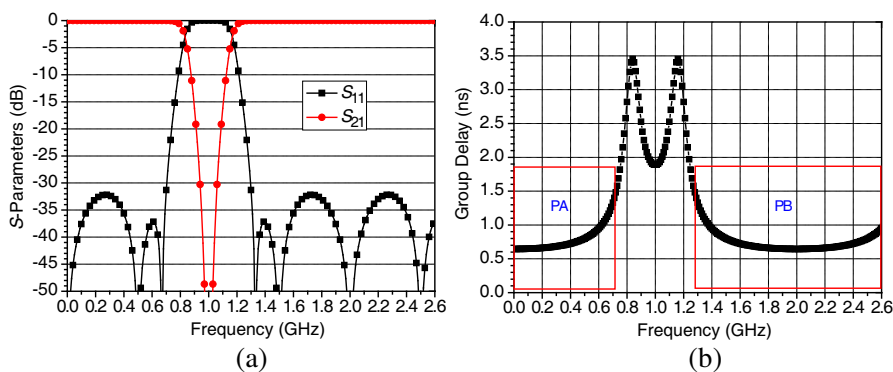


Figure 8. (a) The calculated scattering parameter and (b) group delay performance of the chosen two-section two-cell coupled-line bandstop filter example.

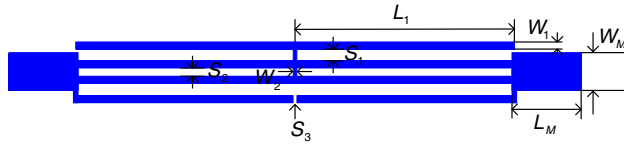


Figure 9. The microstrip layout of the chosen two-section two-cell coupled-line bandstop filter example.

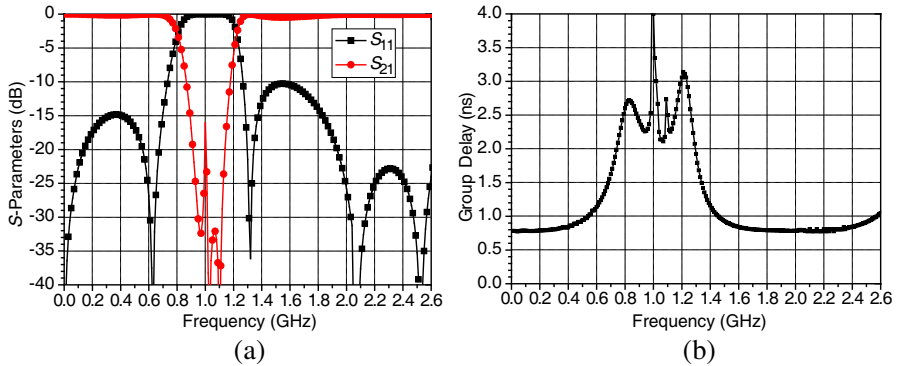


Figure 10. The full-wave simulated responses of the chosen two-section two-cell coupled-line bandstop filter example.



Figure 11. The photograph of the fabricated microstrip bandstop filter.

Figure 11. The corresponding measured responses including scattering parameters, the group delay of the low pass band, and the group delay of the upper pass band are plotted in Figures 12(a), (b), and (c), respectively. As shown in Figure 12(a), the attenuation levels in the band from 0.88 to 1.11 GHz are larger than 20 dB. The measured maximum attenuation level is -37.7 dB at 0.99 GHz (very close to the ideal 1 GHz). The measured out-of-band return loss in the range of 0 to 0.67 GHz is larger than 20 dB while the measured out-of-band return loss in the range of 1.24 to 2.6 GHz is larger than 12 dB. In addition, two transmission poles (or reflection zeros) close to the stop-band edges can be clearly observed in Figure 12(a). The pass-band insertion loss is smaller than 0.66 dB in the range of 0 to 0.67 GHz and smaller than

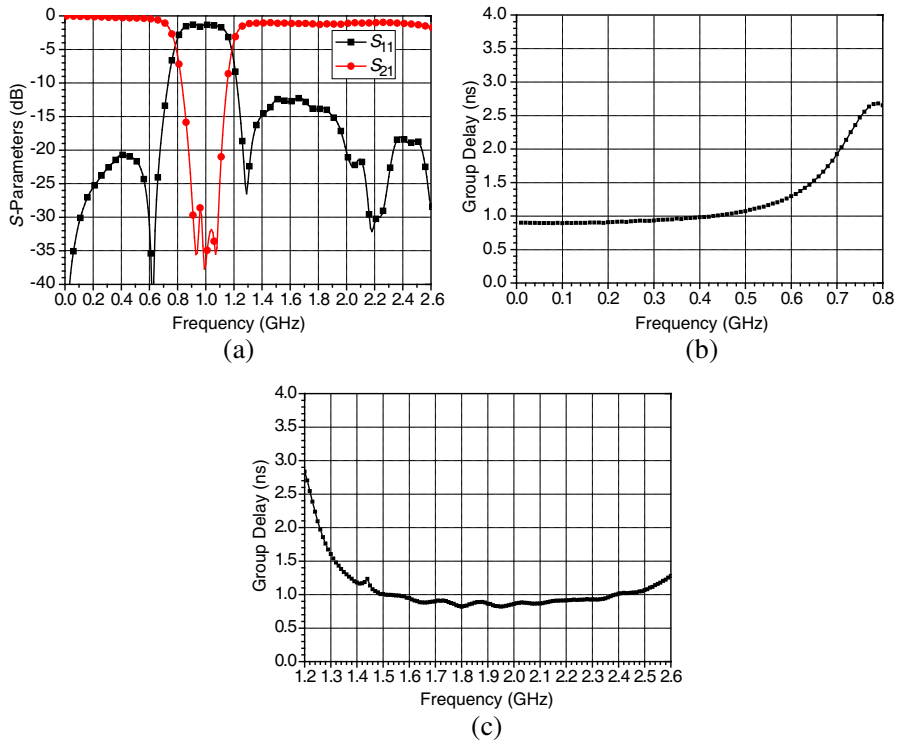


Figure 12. The measured responses of the fabricated microstrip bandstop filter: (a) scattering parameters, (b) the group delay of the low pass band, (c) the group delay of the upper pass band.

1.91 dB in the range of 1.24 to 2.6 GHz. As shown in Figures 12(b) and (c), the maximum (minimum) group delay in the range of 0 to 0.67 GHz is 1.66 ns (0.89 ns) while the maximum (minimum) group delay in the range of 1.24 to 2.6 GHz is 2.24 ns (0.82 ns). In general, the experimental results support our proposed circuit structure and the corresponding synthesis theory.

4. CONCLUSION

A new approach to the design of a compact bandstop filter with sharp skirt selectivity has been presented. The analytical design equations for evaluation of circuit parameters and scattering parameters have been formulated. Excellent performances including large return loss, low insertion loss, sharp skirt selectivity, high attenuation level, and smooth group delay have been demonstrated. For verification, a

two-section two-cell microstrip bandstop filter has been simulated and implemented. The full-wave simulation and experimental results verified that a stop band with sharp skirt selectivity can be obtained in the proposed compact in-line coupled-line circuit structure. In addition, two transmission poles (or reflection zeros) have been observed near the stop-band edges. Finally, note that it is very easy to design high-order bandstop filters by cascading this kind of in-line coupled-line structures. It is expected that this kind of coupled-line bandstop filter can be applied in microwave systems due to the simple in-line configuration and excellent performance.

ACKNOWLEDGMENT

This material is based upon work funded by Zhejiang Provincial Natural Science Foundation of China under Grant No. LY12F04002.

REFERENCES

1. Hong J.-S. and M. J. Lancaster, *Microstrip Filters for RF/Microwave Applications*, Chapters 2 and 6, Wiley, New York, 2001.
2. Chin, K.-S. and C.-K. Lung, "Miniaturized microstrip dual-band bandstop filters using tri-section stepped-impedance resonators," *Progress In Electromagnetics Research C*, Vol. 10, 37–48, 2009.
3. Ning, H., J. Wang, Q. Xiong, and L.-F. Mao, "Design of planar dual and triple narrow-band bandstop filters with independently controlled stopbands and improved spurious response," *Progress In Electromagnetics Research*, Vol. 131, 259–274, 2012.
4. Cheng, D., H.-C. Yin, and H.-X. Zheng, "A compact dual-band bandstop filter with defected microstrip slot," *Journal of Electromagnetic Waves and Applications*, Vol. 26, No. 10, 1374–1380, 2012.
5. Wang, J., H. Ning, Q. Xiong, M. Li, and L.-F. Mao, "A novel miniaturized dual-band bandstop filter using dual-plane defected structures," *Progress In Electromagnetics Research*, Vol. 134, 397–417, 2013.
6. Han, S., X.-L. Wang, and Y. Fan, "Analysis and design of multiple-band bandstop filters," *Progress In Electromagnetics Research*, Vol. 70, 297–306, 2007.
7. Zhang, X.-Y., C.-H. Chan, Q. Xue, and B.-J. Hu, "RF tunable bandstop filters with constant bandwidth based on a doublet configuration," *IEEE Transactions on Industrial Electronics*, Vol. 59, No. 2, 1257–1265, 2012.

8. Ou, Y.-C. and G. M. Rebeiz, "Lumped-element fully tunable bandstop filters for cognitive radio applications," *IEEE Transactions on Microwave Theory and Techniques*, Vol. 59, No. 10, Part 1, 2461–2468, 2011.
9. Xiang, Q.-Y., Q.-Y. Feng, and X.-G. Huang, "A novel microstrip bandstop filter and its application to reconfigurable filter," *Journal of Electromagnetic Waves and Applications*, Vol. 26, Nos. 8–9, 1039–1047, 2012.
10. Wu Y., Y. Liu, S. Li, and C. Yu, "A simple microstrip bandpass filter with analytical design theory and sharp skirt selectivity," *Journal of Electromagnetic Waves and Applications*, Vol. 25, Nos. 8–9, 1253–1263, 2011.
11. Wu, Y., Y. Liu, S. Li, and S. Li, "A novel high-power amplifier using a generalized coupled-line transformer with inherent DC-block function," *Progress In Electromagnetics Research*, Vol. 119, 171–190, 2011.
12. Cui, D., Y. Liu, Y. Wu, S. Li, and C. Yu, "A compact bandstop filter based on two meandered parallel-coupled lines," *Progress In Electromagnetics Research*, Vol. 121, 271–279, 2011.
13. Mandal, M. K., K. Divyabramham, and V. K. Velidi, "Compact wideband bandstop filter with five transmission zeros," *IEEE Microwave and Wireless Components Letters*, Vol. 22, No. 1, 4–6, 2012.
14. Qian, K. W. and X. H. Tang, "Compact bandstop filter using coupled-line section," *Electronics Letters*, Vol. 47, No. 8, 505–506, 2011.
15. Xiang, Q.-Y., Q.-Y. Feng, and X.-G. Huang, "Bandstop filter based on complementary split ring resonators defected microstrip structure," *Journal of Electromagnetic Waves and Applications*, Vol. 25, No. 13, 1895–1908, 2011.
16. Tang, W. and J.-S. Hong, "Coupled stepped-impedance-resonator bandstop filter," *IET Microwaves, Antennas & Propagation*, Vol. 4, No. 9, 1283–1289, 2010.
17. Wu, Y. and Y. Liu, "A coupled-line band-stop filter with three-section transmission-line stubs and wide upper pass-band performance," *Progress In Electromagnetics Research*, Vol. 119, 407–421, 2011.